

IONIZATION OF ARGON BY ATOMS, AND SINGLY OR DOUBLY CHARGED IONS OF NEON AND ARGON

V. V. AFROSIMOV, R. N. IL'IN, V. A. OPARIN, E. S. SOLOV'EV, and N. V. FEDORENKO

Leningrad Physico-Technical Institute, Academy of Sciences, U.S.S.R.

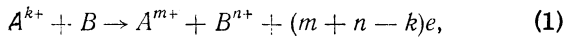
Submitted to JETP editor May 13, 1961

J. Exptl. Theoret. Phys. (U.S.S.R.) 41, 1048-1055 (October, 1961)

The total ionization cross section σ_- and the total cross sections σ_{0n} for the production of slow ions with charges $n = 1, 2, 3, 4$ are measured in the ionization of argon by 20 - 180 keV Ne and Ar atoms and Ne^+ and Ar^+ ions, and by 20 - 360 keV Ne^{2+} and Ar^{2+} ions. σ_- decreases with increasing fast-particle charge. This is accounted for by the decreasing probability of fast-particle stripping with increasing charge. The yield of slow multiply-charged ions increases with the charge of fast incident particles. Charge exchange and ionization with pickup apparently make the principal contributions to the cross section for slow multiply-charged ion production.

INTRODUCTION

INELASTIC atomic collisions accompanied by charge exchange can be described in general by



where A is the incident particle with charge k before and charge m after the collision, and B is a gas atom transformed by the collision into an ion with charge n. We shall designate the incident particles as fast or primary, while the ions and atoms formed from these primary particles will be called fast secondary particles. Ions formed out of gas target atoms will be called slow ions.* The cross section for process (1) will be denoted by σ_{0n}^{km} , where the upper and lower indices pertain to the charges of the fast and slow particles, respectively.

The widely used potential (or capacitor) method for determining ionization and charge exchange cross sections permits measurement of the total cross section for the production of free electrons, interpreted as the total ionization cross section [2]

$$\sigma_- = \sum_{m,n} (m + n - k) \sigma_{0n}^{km} \quad (2)$$

and the total cross section for slow-ion production (with weighting by charge units)

$$\sigma_+ = \sum_n n \sigma_{0n}, \quad (3)$$

where σ_{0n} is the total cross section for the production of slow ions with charge n (see [3]).

Electrons can be freed both from the target gas atoms and from fast particles. Therefore the total ionization cross section is the sum of the cross sections σ_i for gas ionization and σ_l for fast-particle stripping:

$$\sigma_- = \sigma_l + \sigma_i. \quad (4)$$

Mass-spectrometer methods measure the total cross sections for the production of n-fold charged slow ions out of gas atoms (σ_{0n}), or the total cross sections for the production of fast secondary ions with charge m out of fast primary particles (σ^{km}). These are expressed in terms of partial cross sections by

$$\sigma_{0n} = \sum_m \sigma_{0n}^{km}, \quad \sigma^{km} = \sum_n \sigma_{0n}^{km}. \quad (5)$$

The dependence of the total ionization cross section on the primary-particle charge has not been investigated thoroughly. On the one hand, at high (Mev) energies the theory of collision ionization predicts a quadratic dependence. On the other hand, no definite charge dependence has been found at tens of keV. [3,4,5]

In the present work we have investigated the intermediate region of a few hundred keV, concurrently with measurements of the cross sections σ_{0n} for the production of slow ions with different charges. Argon gas was bombarded with fast Ar, Ar^+ , Ar^{2+} , Ne, Ne^+ , and Ne^{2+} . The cross sections for electron capture by these fast particles

*It was established in [1] that ions, especially multiply-charged ions, resulting from gas ionization can possess energies up to a few percent of the fast primary energy. Although the fraction of these relatively energetic ions is small their presence can reduce somewhat the measured cross sections for the production of multiply-charged ions.

had previously been measured in our laboratory.^[6,7] A comparison of the cross sections for the formation of slow ions and of fast secondary ions can be used to determine the correlation between processes occurring in the shells of both colliding particles. More complete information concerning the relationship of these processes requires a new technique combining mass analysis and a coincidence scheme for registering the colliding particles.

EXPERIMENTAL PROCEDURE

In investigating the total ionization cross section σ_- , the total cross section σ_+ for slow-ion production, and the total cross section σ_{0n} for the production of n -fold charged slow ions, we used the experimental apparatus described in ^[8] and ^[9] in conjunction with devices for producing and registering a fast-atom beam. The apparatus is shown schematically in Fig. 1.

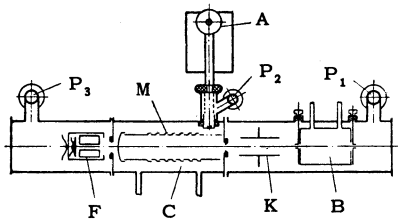


FIG. 1. Experimental apparatus. B – auxiliary charge-exchange chamber, K – capacitor, C – collision chamber, M – measuring capacitor, A – mass analyzer of slow ions, F – fast-particle collector. P_1 , P_2 , and P_3 – pumps.

Fast neutral atoms were produced by resonant charge exchange of a monochromatic ion beam in the auxiliary charge-exchange chamber B, where the gas pressure was $10^{-3} - 10^{-2}$ mm Hg. A pressure differential of the order 1:200 existed between the entrance and exit channels of chamber B. The neutral-atom beam leaving the charge-exchange chamber was cleared of unneutralized fast ions by the electric field of the capacitor K and entered the collision chamber C, which contained a sectional capacitor M for measuring the cross sections σ_- and σ_+ . The cross sections σ_{0n} were determined by the slow-ion analyzer A, which was joined to the collision chamber.

The fast-ion beam intensity was measured by means of the secondary electron emission and was monitored by the thermal effect of the beam in the collector F, which is represented in Fig. 2. The beam impinged on the 15μ thick 20×20 mm grounded nickel foil N. The current of secondary electrons ejected from the foil to the positively biased electrodes E_1 and E_2 was measured. The

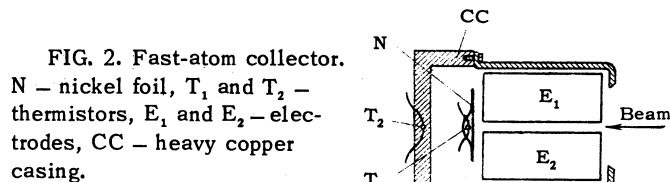


FIG. 2. Fast-atom collector. N – nickel foil, T_1 and T_2 – thermistors, E_1 and E_2 – electrodes, CC – heavy copper casing.

thermistor T_1 was cemented to the back of the foil. The bead thermistor used in the collector was of 0.2 mm diameter, with a temperature coefficient of -4.5% per degree at 20° C. A second identical thermistor T_2 was cemented to the heavy copper casing CC of the collector in order to compensate for the ambient temperature. The two thermistors were incorporated in a bridge for measuring the beam intensity P from the thermistor ratio R_{T_1}/R_{T_2} . The calibration curve $R_{T_1}/R_{T_2} = f(P)$ from which the fast-atom beam intensity was determined had been plotted using a beam of fast singly-charged ions. Control runs showed that $f(P)$ is independent of particle mass and velocity. The thermal-type collector permitted the registration of beam variations as small as 0.1 mw. Beam intensity usually varied in the range 5 – 10 mw.

By means of the thermal collector it was found that the coefficients of secondary-electron emission from the surface of the foil were very close for fast atoms and singly-charged ions of the same element (neon or argon) with identical velocities. It was found more convenient to measure atom-beam intensity by means of secondary-electron emission than with the thermal collector, which is subject to considerable inertia.

A constant check was maintained during all measurements to ensure that the entire beam traversing the collision chamber was also entering the collector located directly behind the chamber.

In the work with ion beams the charge-exchange chamber B was maintained at the extreme vacuum, and the fast-atom collector was used as a Faraday cage consisting of the foil N and the electrodes E_1 and E_2 . In this case a transverse electric field between the electrodes prevented secondary electrons ejected from the foil from leaving the collector. Argon gas pressure in the collision chamber was maintained low at $(2 - 4) \times 10^{-4}$ mm, providing the condition for single scattering. Differential pumping was performed by the pumps P_1 , P_2 , and P_3 . The residual pressure in the collision chamber was $(1 - 2) \times 10^{-6}$ mm.

Random errors incurred in measuring cross sections are estimated at $\pm 12\%$ for fast ions and $\pm 15\%$ for fast atoms.

RESULTS AND DISCUSSION

We measured the total ionization cross section σ_- , the total cross section for slow-ion production σ_+ , and the total cross sections for the production of singly, doubly, triply and quadruply charged slow ions (σ_{01} , σ_{02} , σ_{03} , and σ_{04}) when argon was ionized by fast Ne and Ar atoms and by the ions Ne^+ , Ne^{2+} , Ar^+ , and Ar^{2+} . The energy range for fast atoms and singly charged ions was 20–180 keV; the range for doubly charged ions was 20–360 keV.

 A. Total Ionization Cross Section σ_-

The total cross sections $\sigma_-(v)$ for the ionization of argon by fast Ar atoms and by Ar^+ and Ar^{2+} ions are shown in Fig. 3. Corresponding data for fast Ne atoms and for Ne^+ and Ne^{2+} ions are shown in Fig. 4. σ_- increases monotonically over the entire range to a maximum of the order $(1-1.5) \times 10^{-15} \text{ cm}^2$. This velocity dependence of the ionization cross sections was to be expected, since their maxima must correspond to higher velocities.^[10]

A comparison of the $\sigma_-(v)$ curves for fast ions and atoms of the same element shows a dependence on the fast-particle charge. For the ionization of argon by fast Ne atoms this dependence is exhibited very clearly, beginning at $v \sim 8 \times 10^7 \text{ cm/sec}$. σ_- diminishes with increasing charge.

The observed behavior of σ_- can be accounted for as follows. At low velocities the ion stripping cross section σ_l plays only a small part compared with the gas ionization cross section σ_i . With increasing velocity the stripping contribution to σ_- increases [Eq. (4)], its magnitude being inversely correlated with the fast particle charge. For the

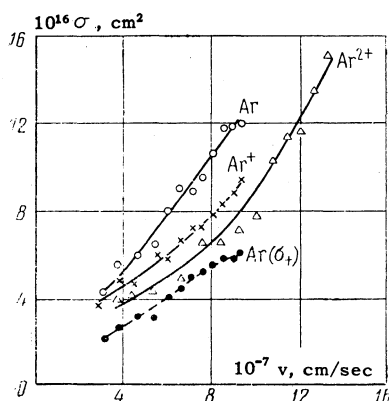


FIG. 3. Velocity dependence of argon ionization cross sections. Solid curves – total ionization cross sections σ_- for fast Ar, Ar^+ , and Ar^{2+} . Dashed curves – total cross section σ_+ for slow-ion production by fast Ar atoms.

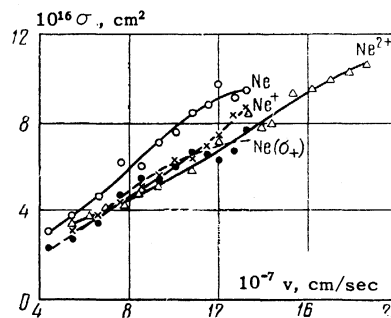


FIG. 4. Velocity dependence of neon ionization cross sections. Solid curves – total ionization cross section σ_- for fast Ne, Ne^+ , and Ne^{2+} . Dashed curves – total cross section σ_+ for slow-ion production by fast Ne atoms.

symmetric Ar-Ar pair, stripping assumes a large role, since electrons must be removed from the shells of both colliding particles with equal probability. Since the equality $\sigma_+ = \sigma_l$ must be fulfilled in gas ionization by fast atoms, we have for the Ar-Ar pair

$$\sigma_l = \sigma_i = \sigma_+ = \sigma_- / 2. \quad (6)$$

The data on σ_+ and σ_- (Fig. 3) for argon ionization by fast argon atoms confirm (6); this is an additional check on the operation of the measuring capacitor. For singly charged fast Ar^+ ions stripping makes a small contribution to σ_- (σ_l is 10–15% of σ_- for Ar^+ -Ar according to^[11]); for Ar^{2+} the contribution should be even smaller. For fast neon ions and atoms the charge dependence of σ_- in the same energy range, i.e., at somewhat higher velocities (Fig. 4), is not so strong as for fast argon particles. This is associated with the fact that neon has higher ionization potentials than argon and smaller stripping cross sections.

A comparison of σ_- for fast argon and neon particles with the same charge and the same velocity (Figs. 3 and 4) shows that the total ionization cross section σ_- is larger for fast particles having a large number of shell electrons. This qualitative conclusion had been reached previously for fast singly charged ions.^[8,10,12]

Firsov^[13] has used statistical concepts to estimate the total ionization cross section in collisions of heavy atomic particles. In Fig. 5 our data are compared with Firsov's universal curve, which is based on his approximate theory that yields cross sections within a factor of 2. The experimental and theoretical cross sections are in agreement within these limits.

In Fig. 6 our results for σ_- in the ionization of argon by Ne^+ are compared with the results given in^[14],^[8], and^[3], and are seen to be in

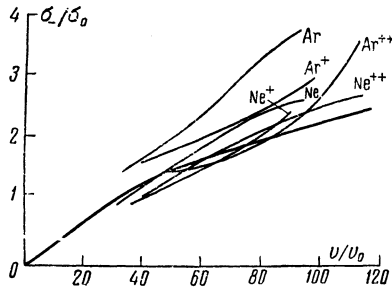


FIG. 5. Total ionization cross sections σ compared with Firsov's theoretical curve (heavy line). The fast primary particles are designated at the end of each experimental curve (thinner lines). v_0 and σ_0 are characteristic values of the velocity and cross section calculated from [13].

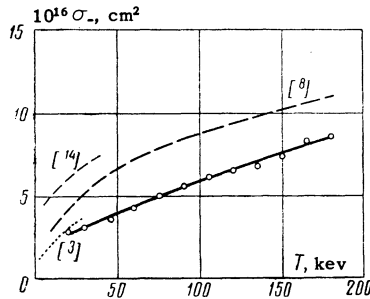


FIG. 6. Total cross sections for argon ionization by Ne^+ given by different authors. The solid curve represents our present work.

best agreement with [3]. The cross section given in [8] exceeds somewhat the experimental error limit in our work and in [3]. The curve in [14] lies considerably above all other curves.

The measurements of σ_- in the ionization of argon by fast Ne and Ar atoms are compared in Fig. 7. Our curve for Ar-Ar agrees well with [5], while for Ne-Ar our results agree with [3] within the limits of error.

The discrepancies between the total ionization cross sections given by different investigators result mainly from the difficulty of excluding extraneous effects while measuring electron currents, and also possibly while measuring gas pressures. The differences between the most recent values given for the cross sections [3, 5, 8] do not exceed $\pm 25 - 30\%$, which is smaller than the discrepancies in earlier work.

B. Total Cross Sections σ_{0n} for the Production of Slow Ions with Different Charges

Figure 8 shows curves of the total cross sections σ_{0n} for the production of slow argon ions with different charges as functions of the velocities of Ar atoms and of Ar^+ and Ar^{2+} ions. Figure 9 shows analogous curves for fast Ne atoms and for Ne^+ and Ne^{2+} ions. The total cross section for the production of slow ions with a given charge is always smaller for fast atoms than for fast ions of the same element. The largest

FIG. 7. Total cross sections for argon ionization by fast Ne and Ar atoms given by different authors. Solid curves – present work; dashed curve – from [3] for Ne-Ar; dash-dot curve – from [5] for Ar-Ar.

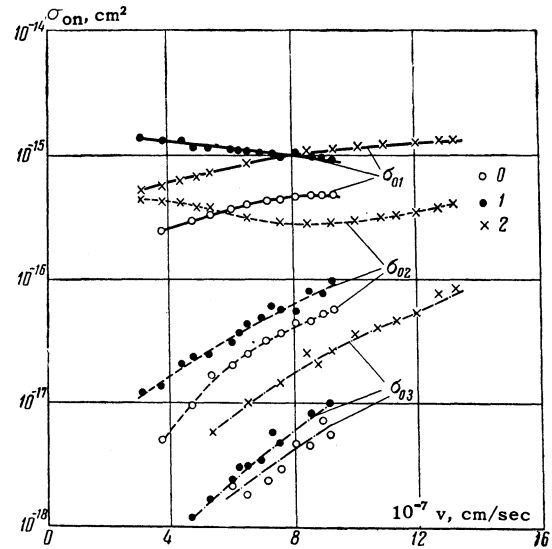
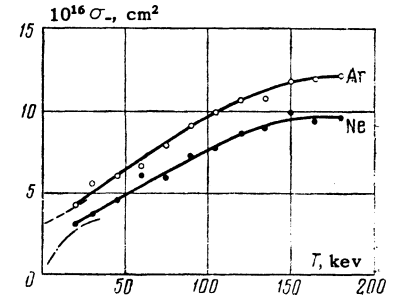


FIG. 8. Total cross sections σ_{01} , σ_{02} , σ_{03} for the production of slow ions with different charges in the ionization of argon by fast Ar, Ar^+ , and Ar^{2+} . The fast-particle charges are identified by the numbers 0, 1, and 2.

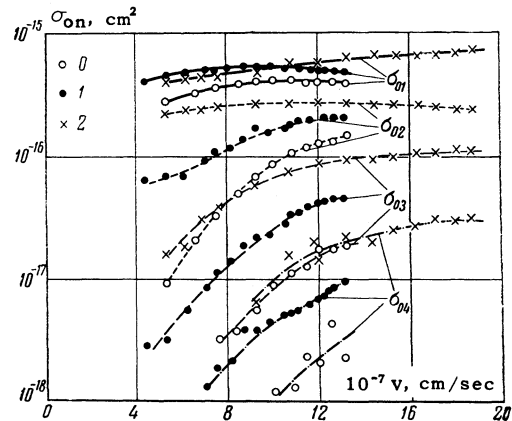


FIG. 9. Total cross sections σ_{01} , σ_{02} , σ_{03} and σ_{04} for the production of slow ions with different charges in the ionization of argon by fast Ne, Ne^+ , and Ne^{2+} . The fast-particle charges are identified by the numbers 0, 1, and 2.

total cross sections for the production of slow ions with charges 2, 3, and 4 are achieved with doubly charged ions.

This basic experimental result can be accounted for as follows. The magnitudes and energy depend-

ences of the cross sections for slow-ion production must reflect the characteristics of the basic processes, which can vary for the different cases. In atom-atom collisions slow ions are produced mainly through pure ionization. In ion-atom collisions analogous cross sections can include a considerable contribution from charge-exchange and from ionization with pickup. It follows from [6] and [7] that charge-exchange processes can possess large cross sections, especially if the fast ions are multiply charged and the charge-exchange process is exothermic. Pure ionization cross sections should increase with velocity up to $v \approx e^2/\hbar$ (electron velocity in the Bohr hydrogen atom). [10] Therefore σ_{0n} in atom-atom collisions increases continuously in the given velocity range. The cross sections for different processes of electron capture by fast ions can either increase or decrease with increasing velocity; therefore the curve of the total cross section $\sigma_{0n}(v)$ in ion-atom collisions can exhibit a minimum.

This situation can be illustrated by comparing some of our curves with those given by Flaks and Solov'ev [6] who measured with mass spectrometers the cross sections for electron capture by fast Ar^{2+} ions in argon. For Ar^{2+} -Ar, Fig. 10 gives our cross sections σ_{01} and σ_{02} , and also σ^{20} and σ^{21} for the production of fast Ar and Ar^+ , respectively, taken from [6]. These four

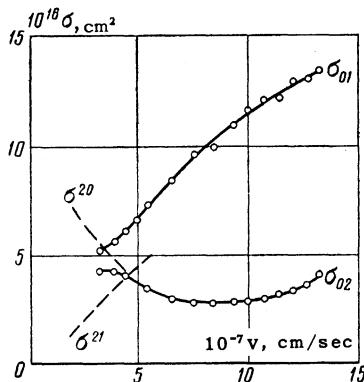


FIG. 10. Total cross sections for the production of slow ions with charges 1 and 2 (σ_{01} and σ_{02}), and cross sections for the production of fast secondary particles (σ^{21} and σ^{20}) in the Ar^{2+} -Ar case. The curves for σ^{21} and σ^{20} were taken from [6].

cross sections can be expressed in terms of partial cross sections for the most probable processes requiring the lowest relative energy expenditure, as follows:

$$\sigma_{01} \approx \sigma_{01}^{22} + \sigma_{01}^{21}, \quad (7)$$

$$\sigma_{02} \approx \sigma_{02}^{22} + \sigma_{02}^{21} + \sigma_{02}^{20}, \quad (8)$$

$$\sigma^{21} \approx \sigma_{01}^{21} + \sigma_{02}^{21}, \quad (9)$$

$$\sigma^{20} \approx \sigma_{02}^{20}, \quad (10)$$

where σ_{01}^{22} and σ_{02}^{22} are the cross sections for pure ionization with the removal of one or two electrons from gas atoms, σ_{01}^{21} is the cross section for single-electron charge exchange, σ_{02}^{21} is the cross section for ionization with single-electron pickup, and σ_{02}^{20} is the cross section for resonant two-electron charge exchange.

In Fig. 10 the lower end of the σ^{20} curve is seen to coincide with the σ_{02} curve. This can occur only if in (8) we have

$$\sigma_{02}^{20} \gg \sigma_{02}^{22} + \sigma_{02}^{21}, \quad (11)$$

i.e., slow doubly-charged argon ions are produced at velocities $v \leq 6 \times 10^7$ cm/sec mainly through resonant two-electron charge exchange. The two other possible processes—ionization with single-electron pickup and pure ionization with the removal of two electrons—are endothermic with an energy expenditure of the order of tens of electron volts. Therefore their contributions to σ_{02} should increase with velocity, leading us to expect the minimum of the $\sigma_{02}(v)$ curve that is actually observed.

The curves for σ_{01} and σ^{21} also exhibit appreciable similarity. These cross sections are of the same order of magnitude and both curves rise, with $\sigma_{01} > \sigma^{21}$ at their intersection. From (7) and (9) we obtain

$$\sigma_{01}^{22} > \sigma_{02}^{21}. \quad (12)$$

The energy expenditure for both processes is of the order of the first ionization potential of argon. However, it seems to us that the inequality of these cross sections reveals a general phenomenological characteristic of inelastic processes that is worth noting. This characteristic is the fact that with the same energy expenditure the less probable process is that in which more electrons participate. The cross section for pure single-electron ionization is on the left in inequality (12), while on the right we have the cross section for ionization with pickup. In the latter process two electrons are removed from the atom, and one of these is captured by the ion, i.e., at least two electrons participate in the process.

In conclusion the authors wish to thank Professor V. M. Dukel'skii for his interest, and I. T. Sheftel' for providing the thermistors and making valuable suggestions regarding their utilization.

¹V. V. Afrosimov and N. V. Fedorenko, ZhTF

27, 2557 (1957), Soviet Phys.-Tech. Phys. **2**, 2378 (1957).

² Il'in, Afrosimov, and Fedorenko, JETP **36**, 41 (1959), Soviet Phys. JETP **9**, 29 (1959).

³ I. P. Flaks, ZhTF **31**, 367 (1961), Soviet Phys.-Tech. Phys. **6**, 263 (1961).

⁴ Fedorenko, Flaks, and Filippenko, JETP **38**, 719 (1960), Soviet Phys. JETP **11**, 519 (1960).

⁵ Sluyters, de Haas, and Kistemaker, Physica **25**, 1376 (1959).

⁶ I. P. Flaks and E. S. Solov'ev, ZhTF **28**, 599 (1958), Soviet Phys.-Tech. Phys. **3**, 564 (1958).

⁷ I. P. Flaks and E. S. Solov'ev, ZhTF **28**, 612 (1958), Soviet Phys.-Tech. Phys. **3**, 577 (1958).

⁸ Fedorenko, Afrosimov, and Kaminker, ZhTF **26**, 1929 (1956), Soviet Phys.-Tech. Phys. **1**, 1861 (1956).

⁹ N. V. Fedorenko and V. V. Afrosimov, ZhTF **26**, 1941 (1956), Soviet Phys.-Tech. Phys. **1**, 1872 (1956).

¹⁰ N. V. Fedorenko, UFN **68**, 481 (1959), Soviet Phys.-Uspekhi **2**, 526 (1960).

¹¹ D. M. Kaminker and N. V. Fedorenko, ZhTF **25**, 1843 (1955).

¹² Afrosimov, Il'in, and Fedorenko, ZhTF **28**, 2266 (1958), Soviet Phys.-Tech. Phys. **3**, 2080 (1958).

¹³ O. B. Firsov, JETP **36**, 1517 (1959), Soviet Phys. JETP **9**, 1076 (1959).

¹⁴ H. B. Gilbody and J. B. Hasted, Proc. Roy. Soc. (London) **A240**, 382 (1957).

Translated by I. Emin

185